Journal of Applied Polymer Science

Lecithin-acrylamido-2-methylpropane sulfonate based crosslinked phospholipid nanoparticles as drug carrier

Esra Cansever Mutlu,[1,2] Muge Sennaroglu Bostan,[3] Fatemeh Bahadori,[4] Abdurrahim Kocyigit,[5] Ebru Toksoy Oner,[1] Mehmet S. Eroglu[3,6]

[1]Department of Bioengineering, Marmara University, Istanbul, Turkey
[2]Scientific Industrial and Technological Application and Research Center, Abant İzzet Baysal University, Bolu, Turkey
[3]Department of Chemical Engineering, Marmara University, Istanbul, Turkey
[4]Department of Pharmaceutical Biotechnology, Bezmialem Vakif University, Istanbul, Turkey
[5]Department of Medical Biochemistry, Bezmialem Vakif University, Istanbul, Turkey
[6]TUBITAK-UME, Chemistry Group Laboratories, Kocaeli, Turkey
Correspondence to: M. S. Eroglu (E-mail: mehmet.eroglu@marmara.edu.tr)

ABSTRACT: In this study, a novel paclitaxel (PTX) loaded and a crosslinked solid phospholipid nanoparticles (SLN-PTX) with negative surface charge was prepared by UV polymerization for drug delivery. Capping of positive charge of zwitterionic lecithin with negative charge of sodium 2-acrylamido-2-methyl-1-propanesulfonate (AMPS-Na) through cation exchange interaction produced a lecithin-AMPS (L-AMPS) complex. The amphiphilic and negative charged lipid complex was emulsified in the presence of emulsifier, paclitaxel, initiator, and methacrylated poly ε-caprolacton-diol (PCL-MAC) as a spacer. The colloidal system was subjected to UV-irradiation to obtain crosslinked nanoparticles. Completion of the UV-polymerization was monitored with differential scanning calorimetry (DSC), which indicated the disappearance of exothermic peaks of vinyl groups. The nanoparticle system, having an average size of 200 nm, exhibited high drug encapsulation (96%) with negatively charged surface (zeta potential had an average of −70 mV). PTX release profiles of the crosslinked and uncrosslinked SLN-PTXs were studied and their pharmacological properties were compared. The crosslinked nanoparticles exhibited more controlled release behavior with longer release time compared to the uncrosslinked ones. *In vitro* cytotoxicity test was conducted on MCF-7 human breast adenocarcinoma cell line, which indicated that the crosslinked SLN-PTXs have a potential therapeutic effect for breast cancer treatments. © 2016 Wiley Periodicals, Inc. J. Appl. Polym. Sci. **2016**, *133*, 44105.

KEYWORDS: biomaterials; drug delivery systems; photopolymerization

Received 5 September 2015; accepted 17 June 2016
DOI: 10.1002/app.44105

INTRODUCTION

Paclitaxel (PTX) was first isolated from bark of a yew tree, *Taxus brevifolia,* in 1967, and since 1979, it has been used as an anti-tumor agent against various tumors.[1–3] PTX is a cytoskeletal drug that binds to β-subunits through the microtubule and promotes the formation of a dysfunctional microtubule structure, resulting in cell death. PTX (C47H51NO14) has a very complex molecular structure possessing a diterpenoid skeleton. Therefore, its semi-synthetic production has become feasible only since 1995. Currently, PTX and its synthetic derivative, docetaxel, are used clinically for the treatment of many cancers types such as breast, ovarian, lung, non-small-cell lung, and Kaposi's sarcoma.[4–7] As PTX is a poorly water-soluble drug, its solubility could only be improved by formulating with amphiphilic drug carrier molecules. They are nanoparticles that overcome biological barriers by reducing toxicity and achieving sustained release of drug by enabling the advantage of the enhanced permeability and retention (EPR) effect.[8–10]

Self-assembly systems, consisting of amphiphilic materials, are one of the best-known and preferred drug delivery systems to deliver hydrophobic therapeutics. The instant formation of spherical particles in aqueous media with an encapsulated drug at the core part is the most favorable behavior of these vehicles. The branched amphiphilic materials are widely utilized to form

Additional Supporting Information may be found in the online version of this article.

firm spheres.[11] Previous reports indicated that while amphiphiles with fewer arms caused the formation of relatively loose particles, the more branched ones made firm spherical particles. Loose drug delivery systems release the cytotoxic payload before reaching the targeted cancer site. However, the most significant disadvantage of highly branched amphiphiles is that the vast amount of polymeric material is injected into a patient during the therapy. Therefore, it is important to synthesize firmly formed spherical drug delivery systems with less armed amphiphiles. Although, crosslinking the amphiphilic arms is known, it is not a well-developed strategy to obtain firmly self-assembled nanoparticles.[12]

A widely used amphiphilic material in preparation of nano drug delivery systems is soybean lecithin, which is a natural zwitterionic phospholipid.[13,14] Its functional derivatives have been widely used in drug delivery applications.[15–18] Although, various solid phospholipid nanoparticle (SLN) formulations have been developed for different therapeutic and diagnostic purposes[16] including anticancer drug delivery,[17–19] immunosuppressant,[20] and peptide delivery,[21] to the best of our knowledge, there is no report available in the literature on the preparation of negatively surface charged and crosslinked lecithin based solid phospholipid nanoparticles (SLNs) for PTX delivery. Date *et al.* prepared self-assembled cationic SLNs by capping negative phosphate groups of soybean lecithin with positively charged cetyl trimethyl ammonium bromide (CTAB) and didodecyldimethylammonium bromide (DDAB).[22,23] These formulations were further used in oral administration of quercetin and anticancer drugs.[24] In this study, a novel strategy has been developed to prepare more stable and crosslinked SLNs for chemotherapeutic delivery of PTX, which relies on the ionic complexation of lecithin with sodium 2-acrylamido-2-methyl-1-propanesulfonate (AMPS-Na) through cation exchange interaction and subsequent UV polymerization and crosslinking. The negatively charged and crosslinked SLNs, with an average size of 200 nm, were found to reach high drug encapsulation performances (96%). Release of PTX from the nanoparticles, which was determined to complete within 14 h, and their pharmacological properties were also investigated. *In vitro* cytotoxicity test was performed on MCF-7 cell line. The PTX containing SLNs, developed in this study, were found to have a high potential as a drug delivery system for breast cancer therapy.

EXPERIMENTAL

Materials

Soybean lecithin was supplied from BDH PROLABO GPR Rectapur and used as received. 2-Acrylamido-2-methylpropane sulfonic acid (AMPS) was supplied from Sigma Aldrich and used as received. A biodegradable polyester, poly(ε-caprolacton)-diol (PCL-diol), (MW 1,250 g/mol) was supplied from Polysciences, Inc., Warrington, PA. Triethylamine (TEA) and methacryloyl chloride were purchased from Sigma-Aldrich. 2,2-Dimethoxy-2-phenylacetophenone (DMPA, 98%,), a photoinitiator, which was used to initialize radical polymerization, was obtained from Sigma-Aldrich. PTX, kindly supplied by DEVA Holding Inc., was produced by Pyhton Biotech Inc. Thirty Slide-A-Lyzer MINI microtubes with a 3,500 Da molecular weight cutoff (Pierce, Rockford, IL) were used for dialysis. All the used solvents were high-pressure liquid chromatography (HPLC) grade and were obtained from Fisher Scientific or Sigma-Aldrich. Phosphate buffer saline (1×PBS, pH = 7.4) was prepared by dissolving 8 g NaCl, 0.2 g KCl, 1.44 g Na2HPO4, and 0.24 g KH2PO4 in 800 mL of ultrapure H2O and the pH was adjusted to 7.4 with HCl. The final volume was fixed to 1 L by adding ultrapure H2O and subsequently sterilized by autoclaving. All the reagents were used without further purification and all the solvents were reagent grade.

Characterization

Fourier transform infrared (FTIR) spectra of the samples were recorded on a Thermo Nicolet 6700 FTIR spectrophotometer equipped with Smart Orbit high performance diamond attenuated total reflectance (ATR) accessories. Measurements were conducted across a range of 400–4,000 cm^{-1} in transmission mode. Nuclear magnetic resonance (NMR) spectra were recorded on a Varian 600 MHz NMR in $CDCl_3$ at room temperature. Proton chemical shifts were recorded in ppm downfield in tetramethylsilane (TMS). Critical micelle concentration (CMC) values of lecithin and Lecithin-AMPS (L-AMPS) ionic complex were determined by fluorescence spectroscopy in aqueous media using FS2 model fluorescence spectrophotometer (Scinco) with a FloroMaster FS-2 software. Particle size and distribution of the samples were determined at 25 °C using dynamic light scattering (DLS) measurements. A Nano-ZS Zen 3600 (Malvern, UK) model DLS instrument with a laser diode illuminated light scattering sensor was used. The average of three measurements was used to represent the intensity (%) distribution of the nanoparticles. Drug loading and release profiles of PTX from the nanoparticles were determined by measuring specific fluorescence emission peak intensities of PTX, using a Molecular Devices SpectraMax 340PC Elisa Reader Spectrophotometer. Scanning electron microscopy (SEM) images of the samples were recorded by SEM Jeol JSM-5910 LV (Tokyo, Japan) at 20 kV. The nanoparticles were isolated from the dispersion by centrifugation and freeze-drying. Images were obtained after sputter coating the nanoparticles in vacuum with a thin layer of gold. XSEM image were recorded to explain if liposomes rather than SLNs were formed. For cross-sectional SEM (XSEM) analysis, freeze dried crosslinked SLN-PTXs were added to a solution of poly(vinylacetate) in methanol and the mixture was poured into Teflon mold to have a polymeric thin film, which was cut up using a razor blade, and the XSEM images were recorded from the sidewall. Transmission electron microscopy (TEM) images of the samples were obtained using a JEOL JEM 2100, operated at acceleration voltage of 200 kV. Differential scanning calorimetry (DSC) was used to determine the extent of polymerization in nanoparticles and phase transition behavior of PTX and the other components. A Perkin Elmer Jade type DSC was used under dynamic argon atmosphere (20 mL/min) at 10 °C/min heating rate. Temperature calibration of the instrument was conducted according to the indium melting point and enthalpy. Test samples were lyophilized and well dried prior to use.

Preparation of Lecithin-AMPS (L-AMPS) Ionic Complex

AMPS was neutralized with sodium carbonate and its pH was brought to 8.0 to obtain sodium salt of AMPS (AMPS-Na).

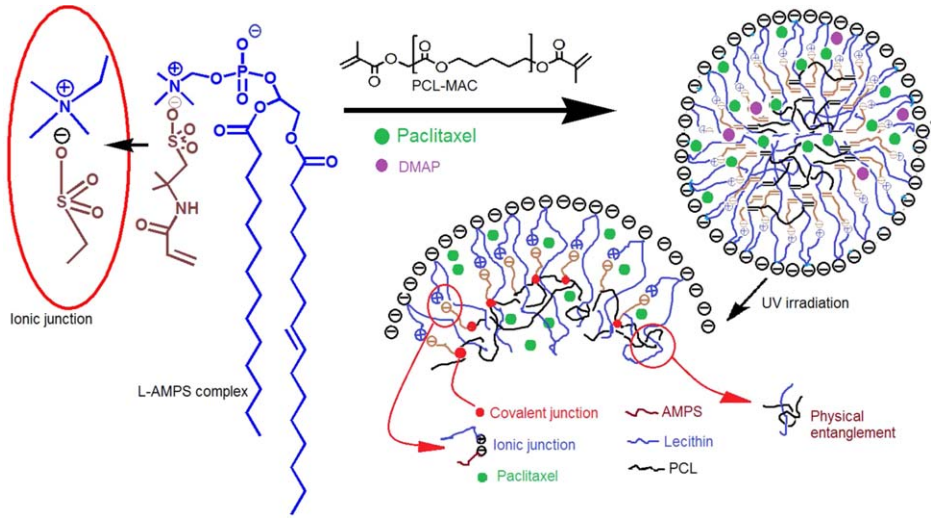

Scheme 1. Preparation mechanism of the PTX loaded nanoparticles. [Color figure can be viewed in the online issue, which is available at wileyonlinelibrary.com.]

Then, 5 mL of 0.13 *M* soybean lecithin and 0.92 *M* AMPS-Na aqueous solutions were mixed by vortexing for 30 min at room temperature. After passing the solution through a coarse filter paper (Macherey-Nagel, 751/75/20, Germany), it was lyophilized to establish cation exchange interaction.[25] The formed L-AMPS ionic complex was extracted with dichloromethane (DCM), and the product was characterized using FTIR and NMR techniques.

Synthesis of Methacrylated Poly(ε-caprolacton diol PCL-diol is erased) (PCL-MAC)

PCL-MAC was used as hydrophobic spacer to increase drug-loading capacity. It was synthesized by methacrylation of PCL-diol in dry DCM at room temperature using a three-necked (250 mL) reactor sealed with rubber septa and equipped with magnetic stirrer and condenser. To a solution of PCL-diol (20 mmol) in DCM (40 mL, dry), 10 mL of TEA was added as catalyst and the reactor was immersed into an ice bath. A solution of methacryloyl chloride (5.22 g, 50 mmol) in DCM (10 mL, dry) was slowly added to the reaction within 30 min and vigorously stirred under argon atmosphere. Then, the reaction mixture was left stirring at room temperature for overnight in dark. The product was isolated after washing with 15% HCI (two times), extracting with DMC, and then precipitating from petroleum ether. Conversion was evaluated using 1H-NMR.

Determination of Critical Micelle Concentration (CMC)

CMC values of both lecithin and L-AMPS samples were determined by fluorescence spectroscopy. The variation in emission (excited at 310 nm) band intensity ratios of pyrene at 383 (I_3) and 373 nm I_1 was determined as a function of lecithin and L-AMPS concentrations (I_3/I_1).[26] For each sample, 30 pyrene solutions in acetone (6 × 10–7 mol/L) were prepared in 1.0 mL vials, and the solvents were evaporated to obtain a thin film of pyrene at the bottom of each vial. L-AMPS solutions, prepared at different concentrations (C1: 90 mg/mL diluted to ¾ proportion up to C30: 2.86 × 10–6 mg/mL) were added to the dried pyrene films, vortexed for 2 min, sonicated for 5 min and subsequently kept at room temperature for 2 h to obtain stable micelles. The ratio of emission peak intensities of pyrene (I_3/I_1) were used to determine CMC values.

Preparation of PTX Loaded Crosslinked Solid Phospholipid Nanoparticles (SLN-PTXs) and Crosslinked Solid Phospholipid Nanoparticles (SLNs)

To a 250 mL round bottom (RB) flask, a mixture of L-AMPS and PCL-MAC (7.8 mg, L-AMPS/PCL-MAC weight ratio 6/1.8), UV initiator (0.078 mg, 1% of L-AMPS, and PCL-MAC mixture), and tween-80 (0.3 mg) as an emulsifier were added. Based on the amount of PCL-MAC, to the mixture, predetermined amounts of PTX were introduced. All the content was dissolved in DCM and mixed for 1 h at room temperature in dark. The solvent was then removed by rotary evaporation to form a thin and dry film in the inner wall of the RB flask. After further drying under vacuum for overnight, 20 mL of ultrapure water was added to the RB flask and subsequently vortexed for 30 min, shaken at 200 rpm for 30 min, and sonicated for 5 min at room temperature. Then, the emulsion was irradiated with UV for 4 h to obtain crosslinked and PXT loaded SLNs. 300/E27/Ultra Vitalux OSRAM Sun Lamp was used for UV polymerization. The crosslinked nanoparticles, not containing PTX (crosslinked SLNs), were prepared as reference samples for release and cell experiments using the same procedure. Furthermore, to observe the effect of crosslinking on particle stability and drug release profile, PTX containing but uncrosslinked nanoparticles were prepared applying the same method, except UV irradiation. Schematic representation of the procedure for SLN-PTXs preparation is designated as in Scheme 1.

Paclitaxel Loading and Release Studies

Initially, a standard calibration curve was obtained using PTX solutions ranging from 0 to 0.9 μg/mL in PBS/acetonitrile (1/10) solution ($R^2 = 0.994$). For release profile of PTX, SLN-PTX suspensions were lyophilized, weighed, and re-suspended in phosphate buffer saline (PBS, pH 7.4) at a concentration of

5 mg/mL. The suspension sample (2 mL) was transferred into a Slide-A-Lyzer MINI dialysis microtube having a molecular weight cutoff of 3,500 Da (Pierce, Rockford, IL) and dialyzed against 45 mL of PBS buffer at 37 °C with a gentle stirring. About 3 mL of aliquots from the dialysis medium were taken at 0.5, 1, 2, 3, 4, 6, 8, 10, 12, and 24 h intervals, which was followed by renewal of the PBS buffer. The amount of free PTX in dialysis medium was determined using a fluorescence and absorbance Elisa reader spectrophotometer by measuring specific emission peak intensities of PTX at 440 nm on excitation at 390 nm. It was previously reported that the release profile of fluorescence anticancer drugs can be monitored using an Elisa reader.[27,28] The percentage of drug release was plotted against time. The samples collected at time intervals and 3 mL of the remaining suspensions in the microtubes were diluted with acetonitrile in ratio of 1/10 (PBS/Acetonitrile) to disassemble the nanoparticles. After the burst release, drug loading and encapsulation efficiency of the nanoparticles were calculated according to the following equations. The tests were performed in triplicate and the results were averaged.

$$\text{Encapsulation efficiency (\%)} = \frac{\text{Weight of PTX in particle}}{\text{Weight of PTX fed initially}} \times 100 \quad (1)$$

$$\text{Drug loading efficiency (\%)} = \frac{\text{Weight of PTX in Particle}}{\text{Weight of PTX in particle} + \text{Weight of lipid fed initially}} \times 100 \quad (2)$$

In Vitro Cytotoxicity of Nanoparticles

Cytotoxic activity assay was performed using Sulforhodamine B method on MCF-7 human breast adenocarcinoma cell line to evaluate *in vitro* activity of crosslinked SLN-PTX formulation. The cell line was maintained in Dulbecco's modified eagle medium of 10% fetal bovine serum and 1% antibiotics (penicillin and streptomycin) under 5% carbon dioxide humidified atmosphere at 37 °C. The optimum formulation of PTX, determined by DLS assay, was obtained by incorporation of PTX in phospholipid based solid lipid nanoparticles (SLNPs) in the ratio of 31.5%, in which, PCL-MAC/L-AMPS ratio was 3/10. This optimum formulation was used as template composition and a series of dilution of PBS was performed to obtain final PTX (in SLNP) concentration ranging from 20 to 0.4 μg/mL. Our studies showed that this dilution in PBS does not make any significant change in the particle size of SLN-PTX (195 nm in PBS, compared to 200 nm in water. Control samples of PTX in 10% dimethyl sulfoxide (DMSO) were prepared in the same final concentrations. The solvents, consisted of 10% DMSO and PBS and empty SLNP (without PTX), were tested at the highest concentrations used in above dilutions. All the samples were prepared and tested in triplicate. The procedure used for *in vitro* cytotoxic activity test was performed according to the literature report.[29] About 190 μL of cell suspension at a density of 5 × 103 cells/well was plated in a 96-well plate. After that, 10 μL/well of the test solutions and controls were added to well culture plates, which were then incubated for 3 days,[30–32] after which the cells were fixed to the plates by adding 100 μL/well of cold 20% trichloroacetic acid and incubated for 1 h at 4 °C. The plates were washed, air-dried, and stained with 100 μL/well of 0.4% sulforhodamine B in 1% acetic acid for 30 min. The plates were washed with 1% acetic acid, rinsed, and 10 m*M* Tris buffer (200 μL/well) was added. The optical density was then read at 515 nm,, and the ratio of sample treated cells with non-treated ones were reported as % survival. Their IC50 values were calculated using nonlinear regression analysis (percent survival vs. concentration).

RESULTS AND DISCUSSION

Spectroscopic Characterization of Lecithin-AMPS and PCL-MAC Spacer

Lecithin, which is a zwitterionic phospholipid, possessing a polar head, and two lipid tails, has been widely used in the preparation of drug carrier systems for various purposes. Its structure makes lecithin amphiphilic, and readily emulsifier in water. As its free trimethylammonium end is convenient for modification to prepare a new amphiphilic polymerizable derivative, this end was capped with negative charge of AMPS-Na through cation exchange interaction, and the product was lyophilized. The ionic complex was isolated by DCM extraction. The prepared negatively charged L-AMPS ionic complex had two hydrophobic lipid tails, and one polymerizable acrylamide group, which is ionically attached to lecithin. The idealized structure, FTIR, and ^{1}H-NMR spectra of L-AMPS ionic complex are given in Figure 1.

In FTIR spectrum of L-AMPS [Figure 1(a)], a broad peak observed at 3,300–3,500 cm^{-1} is due to the —OH groups of absorbed water and a small shoulder at 3,200 cm^{-1} is due to the N—H group of AMPS. Furthermore, this spectrum indicated strong C═O and P—O—C absorption peaks of lecithin at 1,730 cm^{-1} and 1,045 cm^{-1}, respectively. Characteristic peaks at 1,600 cm^{-1} and 1,320 cm^{-1} are due to the C═O vibration and N—H bending of AMPS, respectively. Two peaks appeared at 1,370 cm^{-1} and 1,350 cm^{-1} are due to the asymmetrical and symmetrical stretching of S═O group of AMPS, respectively. The degree of cation exchange interaction between lecithin and AMPS was quantitatively determined by ^{1}H-NMR [Figure 1(b)]. Integration of the characteristic —$C(CH_3)_2$—N— proton peak of AMPS-Na at 1.53 ppm and the characteristic peaks of lecithin at 3.32 ppm [trimethylammonium, —$N^+(CH_3)_3$] confirmed the attachment of AMPS-Na monomers to nearly all trimethylammonium groups of lecithin *via* cation exchange interaction. Considering the insolubility of hydrophilic AMPS-Na in DCM, the characteristic absorption peaks of AMPS and lecithin in FTIR spectrum and their integrations in ^{1}H-NMR spectrum (Figure 1) could be considered as proof of the formation of stable L-AMPS complex.

PCL-MAC was synthesized by capping the hydroxyl ends of PCL-diol (1,250 g/mol) with methacryloyl chloride. Integration of the characteristic peaks at 5.2 and 6.2 ppm (vinyl ═CH_2), 4.1 ppm (—O—CH_2—), 2.3 ppm (—CH_2—O—), and 1.3 ppm (—CH_2—) in ^{1}H-NMR spectrum of PCL-MAC indicated that all the —OH groups were capped [Figure 1(c)]. Due to the polymerizable vinyl groups at both end, PCL-MAC served not only as a crosslinker in the UV polymerization but also as a spacer

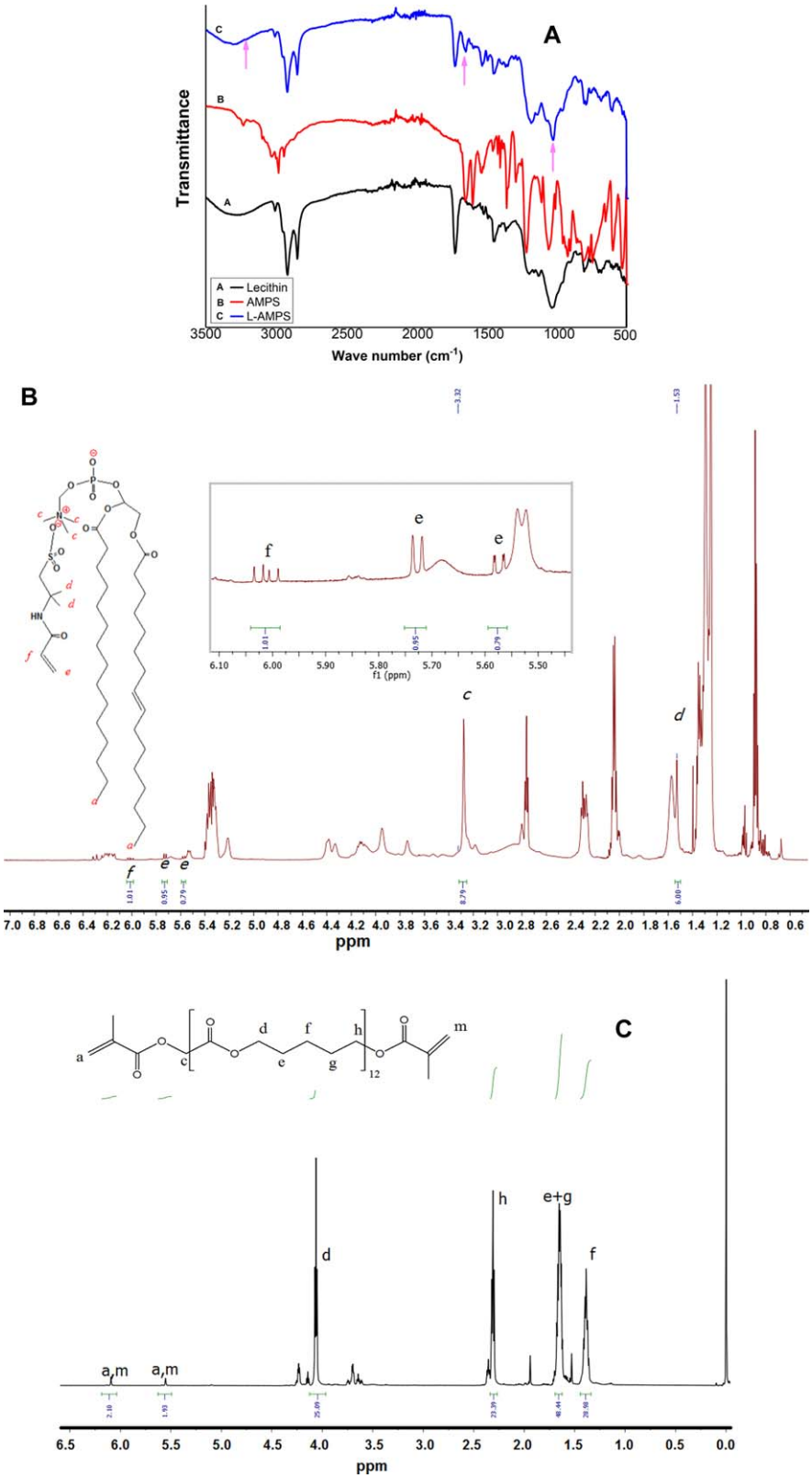

Figure 1. (a) FTIR and (b) ^{1}H-NMR spectrum of L-AMPS ionic complex. (c) ^{1}H-NMR spectrum of PCL-MAC. [Color figure can be viewed in the online issue, which is available at wileyonlinelibrary.com.]

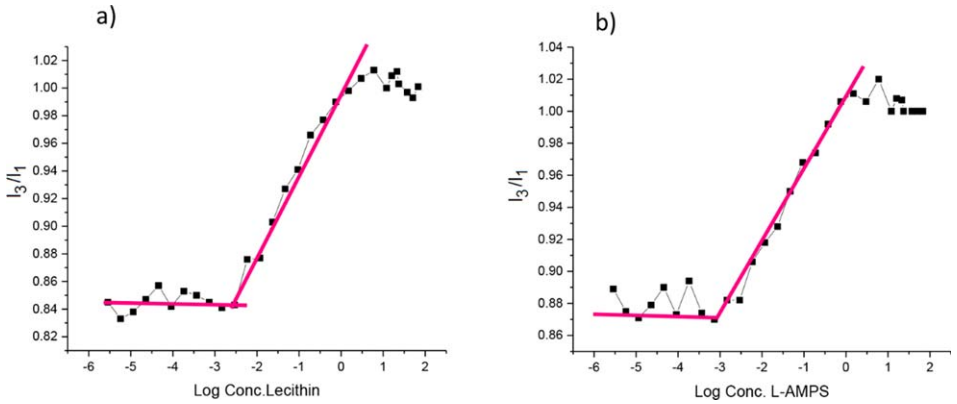

Figure 2. Variation of pyrene I_3/I_1 emission peak intensity ratio with logarithmic concentration (Log C) of (a) Lecithin and (b) L-AMPS complex. [Color figure can be viewed in the online issue, which is available at wileyonlinelibrary.com.]

group. Thus, crosslinked and stable SLNs were obtained after UV irradiation.[33]

Critical Micelle Concentration of Lecithin and L-AMPS Complex

CMC is an important parameter indicating minimum amphiphilic molecule concentration to form stable micelles in water. This was determined by fluorescence spectroscopy using pyrene as fluorophore.[26] Although pyrene is insoluble in water, it is soluble in most of the organic solvents and hydrophobic part of amphiphilic molecules. Below the CMC concentration, there was no micelle present and pyrene had three characteristic emission peaks. The ratio of fluorescence emission peak intensities of the third and first peaks (I_3/I_1) was nearly constant. Over the CMC, with increasing amphiphilic molecule concentration, the I3/I1 peak intensity ratio of pyrene was profoundly increased with increasing solubility of pyrene in the hydrophobic part of the formed micelles. The concentration value of the amphiphilic molecules corresponding to this change was considered as CMC. The changes in the emission peak intensities of pyrene at 383 nm (I3) and 373 nm (I1) were used to determine the CMC of lecithin and L-AMPS complex. Thereby, as shown in Figure 2, $I3/I_1$ ratio values were plotted against the logarithmic concentration of lecithin [Figure 2(a)] and L-AMPS complex [Figure 2(b)]. The concentration value corresponding to the sharp increase in the intensity is taken as CMCs, which was determined as 0.003 mg/mL for lecithin and 0.00074 mg/mL for L-AMPS complex. Elimination of the positive charge of lecithin due to the ionic interaction increased its hydrophobicity and this made lecithin form micelle easier. Lecithin is obtained from various natural sources such as egg yolk, soya bean, etc., with varying length of hydrophobic tiles and thus, CMC values change from 0.2 to 15 m*M*.[34] The CMC value of lecithin determined using pyrene fluorophore is consistent with the literature value. The notable decrease in CMC value after cation exchange interaction could be considered as another proof of the formation of stable L-AMPS complex.

Particle Size and Zeta Potential

Average particle size, polydispersity index (PDI) and zeta potential were measured at room temperature. The data were evaluated as intensity (percent) distribution. Before the measurements, the samples were kept for 3 days at room temperature and the measurements were repeated three times for each sample to be sure of the particle size and stability.[35] A series of crosslinked SLN-PTXs having four different L-AMPS/PCL-MAC ratios were synthesized to explain the effect of composition on the particle size and surface charge. As shown in Figure 3, increasing the amount of PCL-MAC, which served as both crosslinker and hydrophobic spacer, led to the increase of particle size and decrease of zeta potential.

This phenomenon made a significant contribution to obtain a better drug loading capacity and stability profile. Considering these results, the most favorable composition for PTX delivery was determined as PCL-MAC/L-AMPS ratio of 0.3. The composition of the nanoparticles and their particle size and zeta potential values were collected in Table I.

While the average particle sizes of crosslinked SLN and SLN-PTX were 320 nm and 200 nm, respectively, zeta potential values did not show significant change. It is worth noting that crosslinked SLN-PTXs possessed lower particle sizes than those

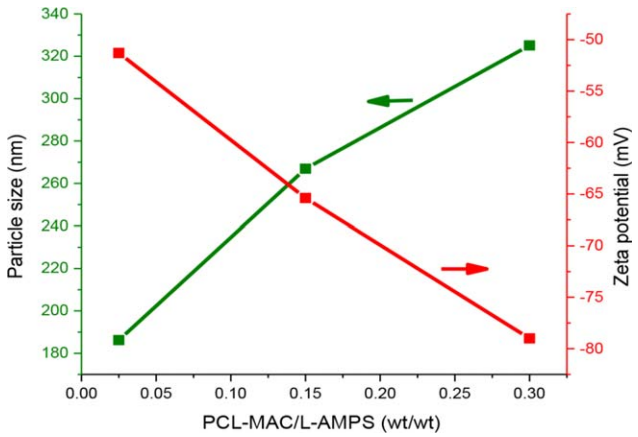

Figure 3. The change of particle size and zeta potential values of crosslinked SLNs with PCL-MAC/L-AMPS weight ratio. Error bars are not added since they are in size of data points. [Color figure can be viewed in the online issue, which is available at wileyonlinelibrary.com.]

Table I. The Nanoparticle Compositions, Their Particle Size as Intensity (Percent), and Zeta Potential Values

Composition (%)	Crosslinked SLN	Crosslinked SLN-PTX	Crosslinked SLN-PTX (Max Load)
L-AMPS (mg)	6.0	6.0	6.0
PCL-MAC (mg)	1.8	1.8	1.8
PTX (mg)	—	0.36	3.6
Tween 80 (mg)	0.3	0.3	0.3
UV initiator (mg)	0.078	0.078	0.078
Average Particle size (nm)	320	200	404
Zeta potential (mV)	−79	−70	−70

of crosslinked SLNs, which could be due to the strong intermolecular interaction between the hydrophobic tail of L-AMPS and PTX. Above a certain PTX concentration, which was 31.5%, nanoparticles did not form.

SEM image and size distribution of the crosslinked SLN-PTXs were determined with their zeta potential and PDI values. As shown in Figure 4(a), all the nanoparticles had a spherical shape. Average particle size, polydispersity index (PDI), and zeta potential value were determined as 200 nm, 0.381, and −70 mv, respectively. To obtain narrow particle size distribution and lower PDI values, the nanoparticle dispersion was centrifuged at different speeds (9,500× g and 85,000× g) and their TEM images were obtained. Particle size distributions became more uniform with lower PDI values as the centrifugation speed was increased [Figure 4(b,c)]. TEM and XSEM images [Figure 4(b,c,d)] showed that the nanoparticles had a very smooth surface, and no drug crystallization with homogenous core was observed, indicating formation of SLNs rather than liposomes.

Characterization of SLN-PTX Formulations Using Differential Scanning Calorimetry (DSC)

Differential scanning calorimetry (DSC) can provide useful information regarding curing reactions, phase transitions, and morphological structure of materials. It has been used extensively in polymer blends and mixtures of low molecular weight compounds to estimate the compatibility and miscibility. The peak areas and the temperatures obtained by DSC are characteristics and quantitative measure of phase transitions. Thus, the completion of a curing reaction and the extent of intermolecular interactions of the components in crosslinked SLN-PTXs were identified by DSC. As shown in Figure 5(a), the melting temperatures of pure components were observed from DSC curves of lecithin ($T_m = 40\,°C$), AMPS-Na ($T_m = 118\,°C$), PCL-

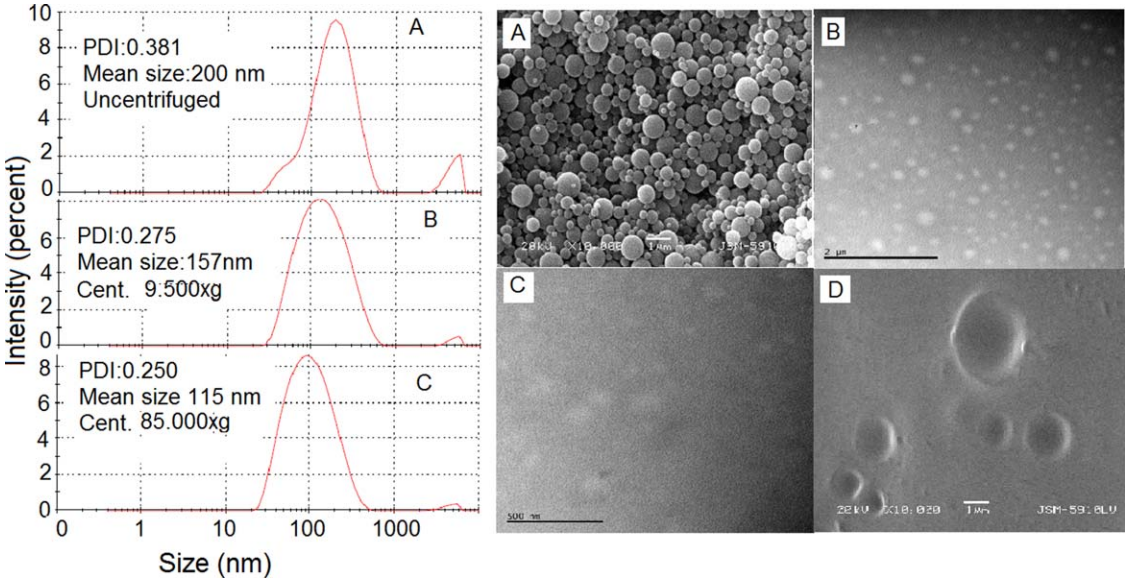

Figure 4. (a) SEM image and size distribution of crosslinked SLN-PTXs. The distribution curves are obtained from DLS measurements, which represent z-average. (31.5% PTX PCL-MAC/L-AMPS ratio is 0.3). TEM images and size distribution of crosslinked SLN-PTXs after centrifugation at (b) 9.500 g; (c) 85.000 g; and (d) XSEM image of PTX loaded nanoparticles in PVAc matrix. This image shows that all particles have uniform and amorphous hydrophobic core. [Color figure can be viewed in the online issue, which is available at wileyonlinelibrary.com.]

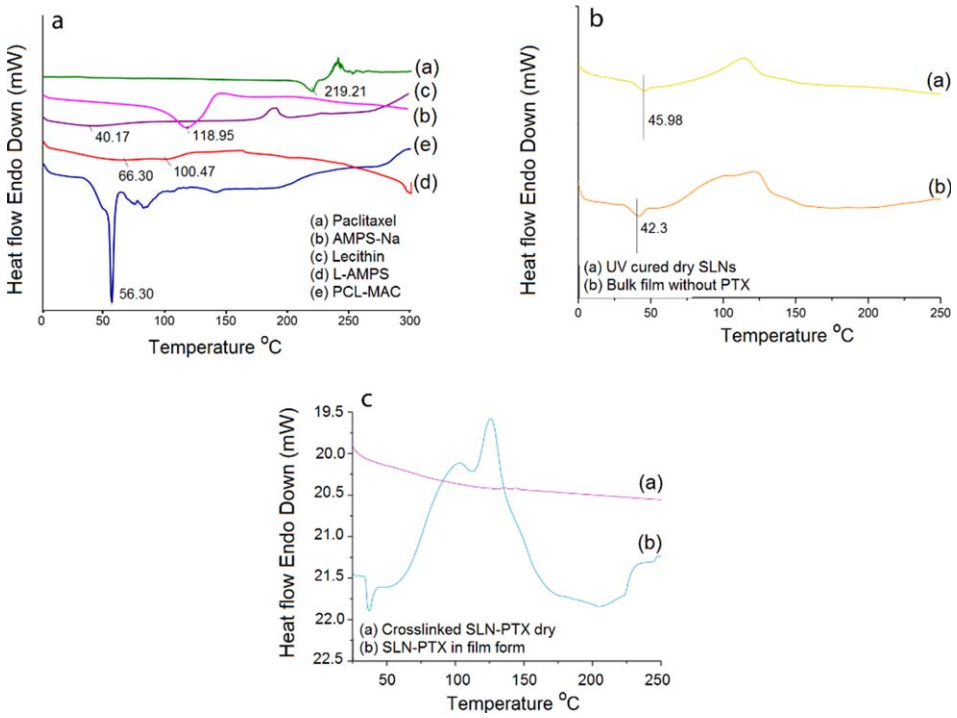

Figure 5. (a) DSC curves of pure components and L-AMPS complex. (b) DSC curves of bulk film without PTX and crosslinked dry SLNs (UV cured nanoparticles were isolated with centrifugation and dried) (c) DSC curves of dry crosslinked SLN-PTXs and dry SLN-PTX formulation in film form. [Color figure can be viewed in the online issue, which is available at wileyonlinelibrary.com.]

MAC ($T_m = 56\,°C$), and PTX ($T_m = 219\,°C$). In this thermogram, L-AMPS complex showed two melting behaviors at 66 °C and 100 °C, which are between melting temperatures of lecithin and AMPS-Na. This is due to the intermolecular interaction between lecithin and AMPS-Na, which is an evidence of the formation of a stable L-AMPS complex.

Additionally, PCL-MAC had the same melting point with PCL-diol, indicating that those terminal methacrylate groups did not influence its crystallization behavior. Figure 5(b) shows the DSC curves of the bulk mixture in dry film form (containing all components except PTX) and crosslinked dry SLNs, which were precipitated by centrifugation and dried before use. In these curves, the melting peaks at 45 and 42 °C are related to PCL-MAC. Interestingly, the melting temperature of PCL-MAC [56 °C in Figure 5(a)] decreased in bulk mixture and in SLNs, which is probably due to the suppression of PCL-MAC crystallinity by hydrophobic interaction with L-AMPS complex. Moreover, another interesting result is the disturbed crystallinity of PTX and PCL-MAC in crosslinked SLN-PTXs by lipid tails of L-AMPS complex [Figure 5(c)]. The DSC curves of the crosslinked SLN-PTXs and PTX incorporated bulk films were recorded to explain the state of PTX in crosslinked SLN-PTXs and the extent of polymerization. The DSC curve of PTX loaded and uncrosslinked bulk film had two distinct exothermic peaks at 110 and 135 °C [Figure 5(c)]. The first peak is due to the exothermic thermal decomposition of UV initiator present in the formulation and the second is due to the polymerization of vinyl groups, which was initiated by the radicals produced by the decomposition of the initiator.[36] In Figure 5(c), the DSC curve of the crosslinked SLN-PTXs had no melting peak, indicating a fully amorphous structure and a uniform distribution of PTX and PCL-MAC in crosslinked SLN-PTXs. It is worth noting that no exothermic peak was observed on the DSC curve up to 250 °C. This is a clear indication of the monomer conversion after the UV irradiation.

PTX Release Study from SLN-PTXs

PTX release from SLN-PTXs was followed using an Elisa reader spectrophotometer by measuring the specific fluorescence emission peak intensities of PTX in PBS at 440 nm. The corresponding concentration values of the peak intensities were obtained from the standard calibration curve and plotted against time. To understand the effect of crosslinking on PTX release profiles, crosslinked and uncrosslinked SLN-PTXs were prepared and their PTX release was followed. The percentage (w/w) release versus time profiles of PTX are shown in Figure 6. Remarkable differences were noticed in PTX release rates of crosslinked and uncrosslinked SLN-PTXs. While nearly all PTX was released from uncrosslinked SLN-PTXs within 6 h, the crosslinked SLN-PTXs displayed prolonged PTX release, which was completed within 14 h and only 15% (w/w) PTX was found to remain in the nanoparticles. The PTX loading and encapsulation efficiencies of crosslinked SLN-PTXs were calculated as 30 and 96% (w/w), respectively. In a previous study, Hu *et al.* have demonstrated that crosslinking by glutaraldehyde decreases the amount of drug released from stearic acid grafted chitosan oligosaccharide micelles. In this study, different degrees of amino

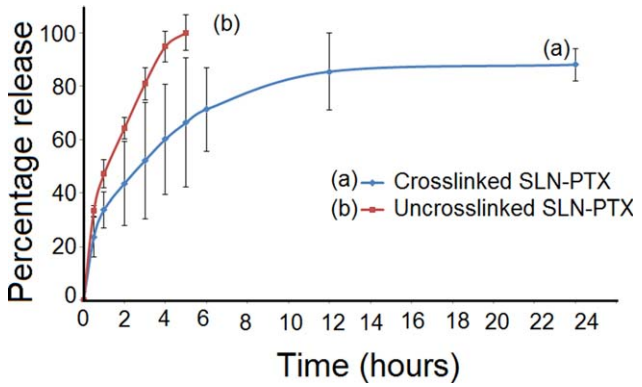

Figure 6. PTX release from crosslinked and uncrosslinked SLN-PTXs. [Color figure can be viewed in the online issue, which is available at wileyonlinelibrary.com.]

substitution has changed the release profile of nano-micelles, however, at the constant degree of amino substitution (42%) the amount of drug released from micelle has decreased from 80 to 50% at the end of 10 h by crosslinking.[37] In another study, core-crosslinked micelles have been developed based on poly(ethylene glycol)-*b*-poly(*N*-2-hydroxypropyl methacrylamide)-lipoic acid (PEG-*b*-PHPMA-LA) conjugates and investigated for triggered doxorubicin (DOX) release. The esterification of the hydroxyl groups in the PEG-*b*-PHPMA copolymers with lipoic acid (LA) has given amphiphilic PEG-*b*-PHPMA-LA conjugates. These micelles have crosslinked with a catalytic amount of dithiothreitol (DTT). The *in vitro* release studies have shown that only about 23.0% of DOX was released in 12 h from crosslinked micelles, whereas about 87.0% of DOX was released.[38] In another study, idarubicin (IDA) and DOX carrying uncrosslinked SLNs, prepared by the similar strategy, was investigated to overcome multiple drug resistance (MDL) in leukemia.[17] In this study, IDA and DOX loading capacities were reported to be 10% (w/w) and 100% of the drugs released within 6 h in PBS at 37 °C. For uncrosslinked SLN-PTXs, we observed nearly the same PTX release rate and higher drug loading capacity (30%, w/w), which is due to the increasing hydrophobicity of the SLNs core with hydrophobic PCL-MAC. Moreover, PTX was released from crosslinked SLN-PTXs within longer time period. By considering the blood circulation time, it is notable that the PTX parenteral delivery within the therapeutic range could be possible by tuning the crosslink density of SLN-PTXs.

In Vitro Cytotoxicity

To determine and compare the cytotoxic activities of the PTX (free drug) and crosslinked SLN-PTXs, the formulations were tested against MCF-7 human breast adenocarcinoma cell line, which was previously used to study the anticancer activity of PTX.[39] Figure 7 presents the cytotoxic activities of free PTX (in 10% DMSO) and crosslinked SLN-PTXs. Both PTX and crosslinked SLN-PTXs exhibited significant and nearly similar cytotoxic activities on MCF-7 cells in 24, 48, and 72 h with the

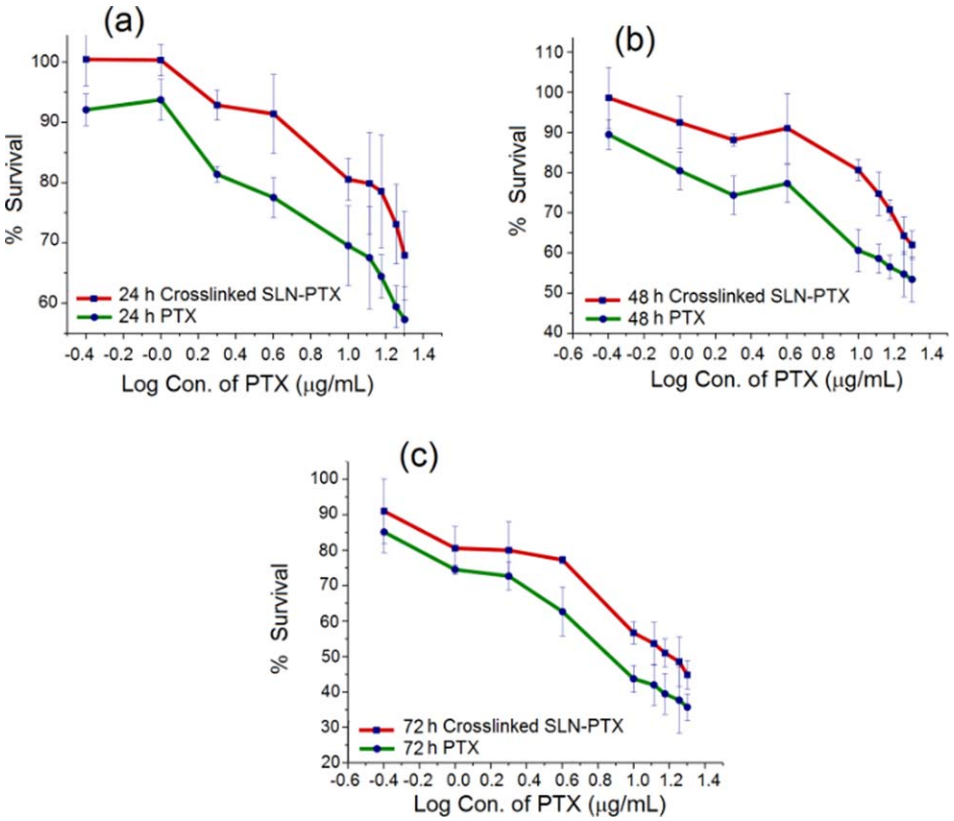

Figure 7. Cytotoxic activities of crosslinked SLN-PTXs and PTX (free drug) after (a) 24 h, (b) 48 h, and (c) 72 h. [Color figure can be viewed in the online issue, which is available at wileyonlinelibrary.com.]

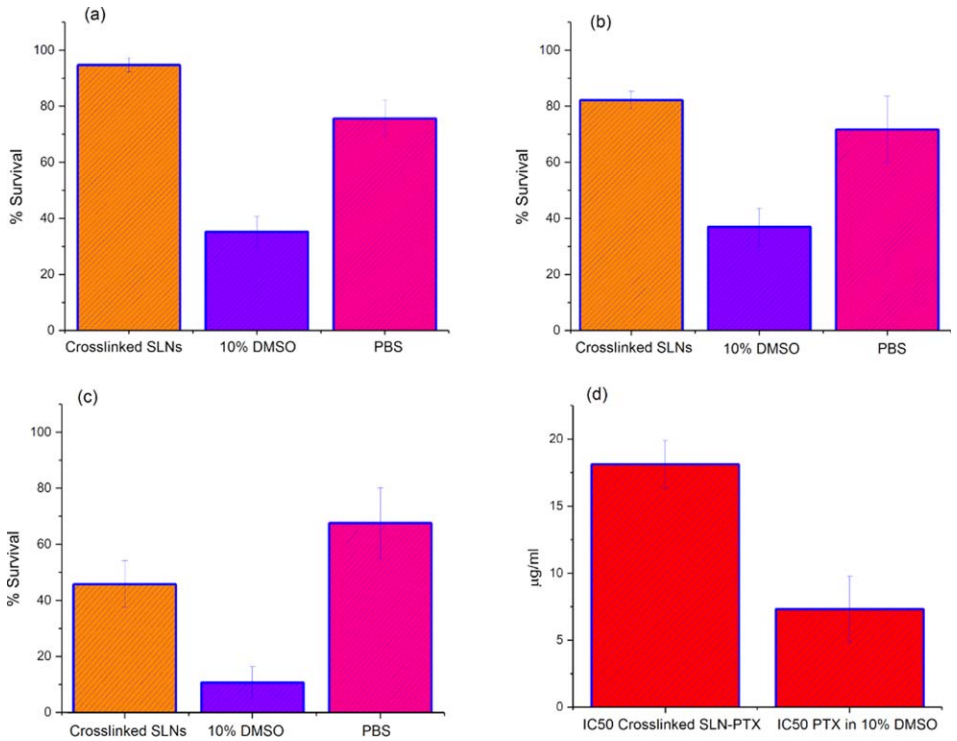

Figure 8. Cytotoxic activity of controls; crosslinked SLNs, DMSO, and PBS after (a) 24 h; (b) 48 h; (c) 72 h; and (d) IC50 values of SLN-PTXs (18.11 µg/mL) and PTX in 10% DMSO (7.3 µg/mL) at the end of 72 h. [Color figure can be viewed in the online issue, which is available at wileyonlinelibrary.com.]

activity of free PTX being the highest one. However, the difference between cytotoxic activity of free PTX and SLN-PTX decreased in time. We hypothesize that the clathrin- and caveoli-mediated endocytosis of the nano-drug delivery system by cancer cells takes a certain period of time and, thus, the cytotoxicity of SLN-PTX approaches to that of free PTX after 72 h.[40]

Dhawan *et al.*[24] prepared cationic SLNs, applying the similar method using ionic complex of lecithin with cetyl trimethyl ammonium bromide (CTAB) and didodecyldimethylammonium bromide (DDAB), by capping negative charge of lecithin with CTAB and DDAB, who studied their cyctotoxic activity and *in vitro* quercetin release. These nanoparticles were reported to have significant selective cytotoxic activity against various cancer cell types. Cytotoxic activity of control groups consisted of crosslinked SLNs (without PTX), 10% DMSO, and PBS, in their highest concentration used in cytotoxicity assay are summarized in Figure 8 along with IC50 values of crosslinked SLN-PTX and free PTX. IC_{50} values of crosslinked SLN-PTXs and free PTX, after 72 h, were found to be 18.11 µg/mL and 7.3 µg/mL, respectively. Considering Figures 7 and 8 together indicates that, SLN does not show significant toxicity at the end of 24 and 48 h, at the highest concentrations applied. This is where SLN-PTX at highest concentrations show 32% and 35% toxicity at the end of 24 and 48 h respectively. As mentioned above, the sudden decrease in viability of cells after 72 h could be attributed to the time, which is needed for the endocytosis of nano drug delivery system by cancer cells. As it could be seen in Figure 8(c), DMSO (10%) is so toxic to MCF-7 cells. Therefore, it is so hard to trust in results obtained from incubation of cells with PTX in 10% DMSO, however, in case of incubating cells with SLN-PTX the conditions are different. The IC_{50} value calculated for crosslinked SLN-PTX corresponds to 18.11 µg/mL PTX (at the end of 72 h). This amount of drug is encapsulated in ≈55 µg/mL of crosslinked SLN [Figure 7(c)]. The highest amount of crosslinked SLN used in this assay was ≈65 µg/mL, which caused 40% of cell viability at the end of 72 h of incubation. Hence, the significant gap between cytotoxicity of crosslinked SLNs with that of crosslinked SLN-PTXs clarifies the success of our novel nanoparticles formulation.

Since the crosslinked SLN-PTXs were exposed to UV light for a certain period of time, the possibility of disrupting the structure of PTX could be argued. Specific fluorescence emission peak of PTX at 440 nm upon excitation at 390 nm, measured for PTX and observed during the drug release study, was concluded as an indication of stability of PTX inside the crosslinked SLN-PTXs. Moreover, the toxic behavior of SLN-PTXs was found to be similar to that of free PTX in terms of the shape, form, and bending of % survival graphs of the crosslinked SLN-PTXs and PTX alone [Figure 7(a–c)]. This evidence again revealed the stability of PTX inside of the crosslinked SLN-PTXs.

CONCLUSIONS

In this study, PTX containing crosslinked SLN-PTXs were prepared by UV polymerization of amphiphilic and negatively charged ionic complex of lecithin-AMPS-Na (L-AMPS), and

their PTX loading capacity, release behavior, and *in vitro* cytotoxicity tests were performed. High drug loading capacity of SLNs was provided by using hydrophobic polymerizable PCL-MAC as a spacer in the core.

Particle size, surface charge, and PDI are the important properties determining the fate of the nanoparticle upon facing the Reticuloendothelial System (RES) rather than material type.[41,42] Generally, the fewer uptakes by RES, the more effectively tumor cells are targeted. Different studies reported that the particles with lower surface charge and sizes smaller than 200 nm promote longer blood residence time. It was also shown that although positively charged particles show a better uptake by cells, the toxicity of these particles against healthy cells is a very important handicap in using them as targeted cancer therapy vehicles.[43] Thus negatively charged spherical particles, as reported in this study, are the ideal carriers for targeting the therapeutic materials to cancer tumors.[44,45] Moreover, it is interesting to note that, the average particle size of crosslinked SLN-PTXs increased up to nearly 32.5% of PTX content and, over this concentration, the nanoparticles did not form. DSC studies showed that the PCL-MAC had a favorable interaction with L-AMPS in the core, and PTX did not crystallize. It was dispersed homogenously into the core because of strong lipid–lipid interaction between PTX and hydrocarbon chains of L-AMPS complex. Cell culture experiments were carried out with MCF-7 human breast cancer cells, which in turn showed that these nano formulations of crosslinked SLN-PTXs had a remarkable potential for human breast cancer treatment.

ACKNOWLEDGMENTS

This study was supported by Marmara University project number BAPKO FEN-C-DRP-101011-0291. ECS gratefully acknowledges the 2211-C Grant provided by the Scientific and Technological Research Council of Turkey (TUBITAK).

REFERENCES

1. Wani, M. C.; Taylor, H. L.; Wall, M. E.; Coggon, P.; McPhail, A. T. *J. Am. Chem. Soc.* **1971**, *93*, 2325.
2. Schiff, P. B.; Fant, J.; Horwitz, S. B. Promotion of Microtubule Assembly In Vitro by Taxol; **1979**, *22*, 277.
3. Spencer, C. M.; Faulds, D. *Drugs* **1994**, *48*, 794.
4. Jordan, M. A.; Wilson, L. *Nat. Rev. Cancer* **2004**, *4*, 253.
5. Wei, Z.; Hao, J.; Yuan, S.; Li, Y.; Juan, W.; Sha, X.; Fang, X. *Int. J. Pharm.* **2009**, *376*, 176.
6. Singla, A. K.; Garg, A.; Aggarwal, D. *Int. J. Pharm.* **2002**, *235*, 179.
7. Friedland, D.; Gorman, G.; Treat, J. *J. Natl. Cancer Inst.* **1993**, *85*, 2036.
8. Kumari, A.; Yadav, S. K.; Yadav, S. C. *Colloids Surf. B* **2010**, *75*, 1.
9. Malam, Y.; Loizidou, M.; Seifalian, A. M. *Trends Pharmacol. Sci.* **2009**, *30*, 592.
10. Peer, D.; Karp, J. M.; Hong, S.; Farokhzad, O. C.; Margalit, R.; Langer, R. *Nat. Nanotechnol.* **2007**, *2*, 751.
11. Wang, F.; Bronich, T. K.; Kabanov, A. V.; Rauh, R. D.; Roovers, J. *Bioconjugate Chem.* **2008**, *19*, 1423.
12. Li, N.; Wang, J.; Yang, X.; Li, L. *Colloids Surf. B* **2011**, *83*, 237.
13. Chan, J. M.; Zhang, L.; Yuet, K. P.; Liao, G.; Rhee, J. W.; Langer, R.; Farokhzad, O. C. *Biomaterials* **2009**, *30*, 1627.
14. Koifman, N.; Schnabel-Lubovsky, M.; Talmon, Y. *J. Phys. Chem. B* **2013**, *117*, 9558.
15. Szuhaj, B. F. Lecithins: Sources, Manufacture, and Uses; The American Oil Chemists Society: Champaign, Illinois, **1989**.
16. Pragati, S.; Kuldeep, S.; Ashok, S.; Satheesh, M. *Int. J. Pharm. Sci. Nanotechnol.* **2009**, *2*, 509.
17. Ma, P.; Dong, X.; Swadley, C. L.; Gupte, A.; Leggas, M.; Ledebur, H. C.; Mumper, R. J. *J. Biomed. Nanotechnol.* **2009**, *5*, 151.
18. Chinsriwongkul, A.; Chareanputtakhun, P.; Ngawhirunpat, T.; Rojanarata, T.; Sila-on, W.; Ruktanonchai, U.; Opanasopit, P. *AAPS Pharm. Sci. Tech.* **2012**, *13*, 150.
19. Wong, H. L.; Rauth, A. M.; Bendayan, R.; Manias, J. L.; Ramaswamy, M.; Liu, Z.; Erhan, S. Z.; Wu, X. Y. *Pharm. Res.* **2006**, *23*, 1574.
20. Kim, S. T.; Jang, D. J.; Kim, J. H.; Park, J. Y.; Lim, J. S.; Lee, S. Y.; Lee, K. M.; Lim, S. J.; Kim, C. K. *Pharmazie* **2009**, *64*, 510.
21. Hu, F. Q.; Hong, Y.; Yuan, H. *Int. J. Pharm.* **2004**, *273*, 29.
22. Date, A. A.; Srivastava, D.; Nagarsenker, M. S.; Mulherkar, R.; Panicker, L.; Aswal, V.; Hassan, P. A.; Steiniger, F.; Thamm, J.; Fahr, A. *Nanomedicine* **2011**, *6*, 1309.
23. Date, A. A.; Nagarsenker, M. S.; Patere, S.; Dhawan, V.; Gude, R. P.; Hassan, P. A.; Aswal, V.; Steiniger, F.; Thamm, J.; Fahr, A. *Mol. Pharmaceutics* **2011**, *8*, 716.
24. Dhawan, V. V.; Joshi, G. V.; Jain, A. S.; Nikam, Y. P.; Gude, R. P.; Mulherkar, R.; Nagarsenker, M. S. *Cell Oncol.* **2014**, *37*, 339.
25. Son, D. H.; Hughes, S. M.; Yin, Y.; Alivisatos, A. P. *Science* **2004**, *306*, 1009.
26. Kalyanasundaram, K.; Thomas, J. *J. Am. Chem. Soc.* **1977**, *99*, 2039.
27. Bahadori, F.; Dag, A.; Durmaz, H.; Cakir, N.; Onyuksel, H.; Tunca, U.; Topcu, G.; Hizal, G. *Polymers* **2014**, *6*, 214.
28. Dong, X.; Mattingly, C. A.; Tseng, M. T.; Cho, M. J.; Liu, Y.; Adams, V. R.; Mumper, R. J. *Cancer Res.* **2009**, *69*, 3918.
29. Krishnadas, A.; Rubinstein, I.; Önyüksel, H. *Pharm. Res.* **2003**, *20*, 297.
30. Önyüksel, H.; Mohanty, P. S.; Rubinstein, I. *Int. J. Pharm.* **2009**, *365*, 157.
31. Önyüksel, H.; Jeon, E.; Rubinstein, I. *Cancer Lett.* **2009**, *274*, 327.
32. Dagar, S.; Krishnadas, A.; Rubinstein, I.; Blend, M. J.; Önyüksel, H. *J. Controlled Release* **2003**, *91*, 123.
33. Berger, J.; Reist, M.; Mayer, J.; Felt, O.; Peppas, N.; Gurny, R. *Eur. J. Pharm. Biopharm.* **2004**, *57*, 19.
34. Walde, P.; Blöchliger, E.; Morigaki, K. *Langmuir* **1999**, *15*, 2346.
35. Vagberg, L. J.; Cogan, K. A.; Gast, A. P. *Macromolecules* **1991**, *24*, 1670.

36. Eroglu, M. S.; Hazer, B.; Baysal, B. M. *J. Appl. Polym. Sci.* **1998**, *68*, 1149.

37. Hu, F. Q.; Ren, G. F.; Yuan, H.; Du, Y. Z.; Zeng, S. *Colloids Surf. B* **2006**, *50*, 97.

38. Wei, R.; Cheng, L.; Zheng, M.; Cheng, R.; Meng, F.; Deng, C.; Zhong, Z. *Biomacromolecules* **2012**, *13*, 2429.

39. Li, C.; Qiu, Y.; Li, X.; Liu, N.; Yao, Z. *Bioorg. Med. Chem. Lett.* **2014**, *24*, 855.

40. Hughes, G. A. *Dis. Mon.* **2005**, *51*, 342.

41. He, C.; Hu, Y.; Yin, L.; Tang, C.; Yin, C. *Biomaterials* **2010**, *31*, 3657.

42. Miller, C. R.; Bondurant, B.; McLean, S. D.; McGovern, K. A.; O'Brien, D. F. *Biochemistry* **1998**, *37*, 12875.

43. Fröhlich, E. *Int. J. Nanomed.* **2012**, *7*, 5577.

44. Kralj, S.; Rojnik, M.; Jagodič, M.; Kos, J.; Makovec, D. *J. Nanoparticle Res.* **2012**, *14*, 1.

45. Bertrand, N.; Wu, J.; Xu, X.; Kamaly, N.; Farokhzad, O. C. *Adv. Drug Delivery Rev.* **2014**, *66*, 2.